A Case Study of Fluid Transport in Shale Crushed Samples: Experiment and Interpretation

Tianhao Wu, Zheng Jiang, Dongxiao Zhang
Energy and Resources Engineering, College of Engineering
Peking University, Beijing, China

This paper was prepared for presentation at the International Symposium of the Society of Core Analysts held in Avignon, France, 8-11 September, 2014

ABSTRACT

Pulse-decay experiment performed on crushed samples has been shown to be a promising method for measuring matrix permeability of extremely low permeable formations, like shale reservoir, since it is much faster than the traditional transient tests performed on core plugs. Due to the fact that the flow of methane in the nanoscale shale matrix involves complex mechanisms, such as the transition flow or slip flow, the physical model plays a key role in reasonable interpretation of experimental data. The objective of this study is to measure the intrinsic permeability of crushed shale samples through pulse-decay experiment, interpret the data with a comprehensive model, including Knudsen diffusion as well as adsorption, and demonstrate the necessity of considering these effects from a new perspective based on molecular dynamics (MD) simulation. The MD simulation addresses the necessity of considering the diffusion and adsorption effects. A more accurate model to calculate shale permeability is applied. By using this model, a significant improvement in the modeling of nanoscale gas flow and interpretation of intrinsic permeability experimental data can be achieved.

This study leads to the following findings: 1) the distribution of gas atoms number density across the nanopore is not uniform, but the gas atoms have the similar self-diffusion velocity, thus a totally different mass flow rate and more complicated mechanisms may appear; 2) the diffusion effect and adsorption effect will change the flow regime and may even dominate the flow regime in ultra-tight porous media; 3) the comprehensive model can describe the flow behavior very well for most of the shale samples; 4) there may exist multi-porous media phenomenon in shale matrix.

INTRODUCTION

Permeability is one of the most fundamental properties for reservoir evaluation and modeling. However, shale permeability has not yet been fully understood because of the complex nanoscale mechanisms and the time consuming experiments. Accurate and fast determination of shale permeability is challenging, in both experimental and theoretical investigations. Traditional steady-state gas permeability test method is not applicable for shale sample because it is time consuming and the flow rate is instable and too small to

detect. Currently, there are two direct methods in common use for determining permeability of extremely tight rocks in the laboratory, namely the transient pulse-decay method using core plug (Dicker et al. 1988; Jones 1997) and the crushed sample method (Luffel et al. 1993; Egermann et al. 2005). Pulse-decay technique on core plug applies a pressure pulse on the upstream end of a confined core and measures the pressure changes in upstream and downstream reservoir, this technique can measure permeability as low as 10^{-9} mD, theoretically (Cui et al. 2009). Pulse-decay experiment performed on crushed samples has been shown to be an alternative for shale formations because it is cheaper and faster than traditional transient technique, although it is restricted to experimental condition in the absence of overburden pressure.

Shale matrix is considered as a kind of highly compacted sediment with an average grain radius of usually smaller than 0.006 cm and complex nanopores (Kundert et al. 2009; Sondergeld et al. 2010). Porosity and permeability in such systems are typically ultralow, and the pore size is thought to be comparable to the mean free path of methane. In this case, the gas – solid interaction has great effects on the flow through the porous media, therefore the widely used first-order Klinkenberg Correction will result in significant deviation, whereas using high-order (e.g. second-order) Klinkenberg correction (Tang et al. 2005; Zhu et al. 2007; Ziarani and Roberto 2012) could lead to a better result. Among the majority of the previous work, one of the most widely accepted approaches is to adopt the conception of intrinsic permeability and apparent permeability and apply the apparent permeability correction factor (Beskok and Karniadakis 1999; Javadpour 2009; Civan 2010; Civan et al. 2011, 2012; Sakhaee-Pour and Bryant 2012). It has been shown that the multi-mechanism, including Knudsen diffusion, slip flow, adsorption, plays critical roles and thus cannot be neglected.

In addition, most of the apparent permeability correlation is based on the correction of continuum flow, the assumption of which is no longer perfectly valid in the nanoscale flow. Under this circumstance, molecular dynamics (MD), which does not require the assumption of continuum flow assumption and models the flow behavior essentially from the physical principles, is another way to understand the microscopic phenomenon. Some results of previous work about MD simulations revealed that considering the density distribution profile of gas molecules will lead to a better agreement with high-order boundary condition of slip flow and experimental results, even suggested that significant adjustment in shale storage capacity calculation is necessary (Zhang et al. 2010; Ambrose et al. 2012).

In this paper, the MD simulation of methane in kerogen is carried out and found to be very helpful for understanding the gas flow mechanisms at microscopic scale in shale formation. As a case study, we investigate shale matrix permeability experimentally and interpret the experimental data with a comprehensive model.

THEORETICAL BACKGROUND

MD simulation of gas transport in nanopores is often achieved by the use of equilibrium MD (EMD) or non-equilibrium MD (NEMD). In order to overcome some disadvantages of traditional EMD and NEMD methods, a dual-control volume grand canonical MD

(DCV-GCMD) method is introduced to investigate the gas transport behavior in nanoscale porous media (Cracknell et al. 1995; Skoulidas et al. 2002). Firouzi and Wilcox (2012, 2013) performed DCV-GCMD simulations of gas flow on carbon-based nanopores. In this study, the EMD simulation of methane is implemented to determine the density distribution and describe gas self-diffusion phenomenon.

In the simulation, the gas molecules are represented by the Lennard-Jones particles, with pair interactions approximated by the LJ potential:

$$u_{LJ} = 4\varepsilon\left[\left(\frac{\sigma}{r}\right)^{12} - \left(\frac{\sigma}{r}\right)^{6}\right] \tag{1}$$

where ε is the depth of the potential well and σ is the finite distance at which the interaction is zero.

The interaction potential between a fluid particle and pore wall is given by the 10-4-3 potential of Steele (Steele 1974):

$$u_{sf} = 2\pi\varepsilon\left[\frac{2}{5}\left(\frac{\sigma_{sf}}{r}\right)^{10} - \left(\frac{\sigma_{sf}}{r}\right)^{4} - \frac{\sigma_{sf}^{4}}{3\Delta\left(0.61\Delta + r\right)^{3}}\right] \tag{2}$$

where Δ is the space between adjacent wall molecular layers and sf denotes solid-fluid interaction.

The procedure and apparatus of permeability test of crush samples is the same with the Helium pycnometer, which is well reviewed by Cui et al. (2009). Gas transport in tight porous rock can be described by diffusion type equation, which assumes that Darcy's law prevails and the measured apparent permeability can be corrected by the Knudsen's correction, with gas pressure or density as the primary unknowns. Therefore, the one-dimensional mass balance equation for a spherical shape particle can be described as follows (Cui et al. 2009):

$$\phi\frac{\partial\rho}{\partial t} + (1-\phi)\frac{\partial q}{\partial r} = \frac{1}{r^2}\frac{\partial}{\partial r}\left(r^2\frac{\rho k_a}{\mu}\frac{\partial p}{\partial t}\right) \tag{3}$$

where ϕ is porosity, ρ is gas density, t is time, q is adsorbate density per unit sample mass, r is displacement or location in the particle, μ is gas viscosity, p is pressure and the apparent permeability k_a is correlated with intrinsic permeability k as follows (Beskok and Karniadakis 1999):

$$k_a = k \cdot f(Kn) \tag{4}$$

where $f(Kn)$ is a dimensionless correction factor determined by

$$f(Kn) = \left(1 + \alpha Kn\right)\left(1 + \frac{4Kn}{1+Kn}\right) \tag{5}$$

where *Kn* is Knudsen number, describing the flow regime which is either slip flow ($0.001 < Kn < 0.1$) or transition flow ($0.1 < Kn < 10$) during a shale permeability test, which is given by:

$$Kn = \frac{\lambda}{R_h} \tag{6}$$

where λ is the molecules' mean free path and R_h is a representative length (mean hydraulic radius of flow tubes in porous media, for example).

The α is the dimensionless rarefaction coefficient whose form and coefficients can be given by Civan et al. (2010).

$$\alpha = \alpha_0 \left(1 + \frac{A}{Kn^B}\right)^{-1}, \quad (\alpha_0 = 1.358; A = 0.1780; B = 0.4348) \tag{7}$$

By rearranging Eq. (3) we have the balance equation with respect to gas density (Cui et al. 2009):

$$\frac{\partial \rho}{\partial t} = \frac{k_a}{\mu c_g \left[\phi + (1-\phi) K_{ad}\right]} \frac{1}{r^2} \frac{\partial}{\partial r}\left(r^2 \frac{\partial \rho}{\partial t}\right) \tag{8}$$

where c_g is the gas compressibility,

$$c_g = \frac{1}{\rho} \frac{d\rho}{dp} \tag{9}$$

and the gas density ρ is given as real gas state of equation $\rho = p / zRT$, and K_{ad} is the derivative of adsorbate density with respect to the gas density.

$$K_{ad} = \frac{\partial q}{\partial \rho} \tag{10}$$

The q is given as Langmuir gas adsorption isotherms:

$$q = V_L \frac{p}{p_L + p} \tag{11}$$

where V_L and p_L are Langmuir volume and pressure, respectively.

By defining apparent transport coefficient K:

$$K = \frac{k_a}{\mu c_g \left[\phi + (1-\phi) K_{ad}\right]} \tag{12}$$

Eq. (3) becomes the diffusion type equation:

$$\frac{\partial \rho}{\partial t} = \frac{K}{r^2}\frac{\partial}{\partial r}\left(r^2 \frac{\partial \rho}{\partial t}\right) \tag{13}$$

For rock particles, the initial and boundary conditions are as follows:

$$\rho = \rho_0 \quad \text{for } 0 \le r < R_a \quad \text{at } t = 0 \tag{14}$$

$$\rho = \rho_{c0} \quad \text{for } r = R_a \quad \text{at } t = 0 \tag{15}$$

$$\frac{\partial \rho}{\partial r} = 0 \quad \text{at r} = 0 \tag{16}$$

$$-4N\pi R_a^2 \frac{k_a}{\mu c_g}\frac{\partial \rho}{\partial r} = V_c \frac{\partial \rho}{\partial t} \quad \text{at r} = R_a \tag{17}$$

where N is the equivalent particle number,

$$N = \frac{3M}{4\rho_b \pi R_a^3} \tag{18}$$

M is the sample mass, R_a is the average particle radius, V_c is the total volume of open space in reference and sample cells (excluding the pore within the sample) , ρ_b is the sample bulk density, ρ_0 is the initial gas density in the sample particles' pore space before gas expansion, and ρ_{c0} is the average initial gas density in the void volume in both sample cell and reference cell when the valve between the sample cell and reference cell is turned on by assuming that the gas reaches equilibrium immediately.

Cui et al. (2009) suggested fitting the permeability through analytical solutions for late-time or early-time technique. However, the analytical solutions are derived under certain assumptions and conditions, which are not suitable for model diagnosis and multi-parameter fitting. Therefore, we use the method proposed by Civan et al. (2012), which determines the best fitted values by matching the simulator-based numerical solution with experimental data. Firstly, this method assumes that different tests marked by $i = 1, 2, ..., X$ are conducted for the same sample. Each sample provides the discrete value of the system's pressure taken at different times marked by $j = 1, 2, ..., Y_i$ for the ith test. Then, this method applies a least-square regression using certain values, e.g. pressure or pressure gradient, calculated by numerical solution and measured values. This objective is accomplished by minimizing the following root-mean-square relative deviation (Civan et al. 2012):

$$E = \sqrt{\frac{1}{XY}\sum_{i=1}^{X}\sum_{j=1}^{Y}\left[1 - \frac{x\big|_{calculated}}{x\big|_{measured}}\right]_{i,j}^2} \tag{19}$$

where x is the specified values which can be chosen according to the model, e.g. gas density in this study.

We can determine parameters $Q_k : k = 1,2,...,S$ of the model described in the preceding paragraphs to minimize the root-mean-square relative deviation given by solving Eq.(19) :

$$\frac{\partial E}{\partial Q_k} = 0, \quad k = 1,2,...,S. \tag{20}$$

Results and Discussion

1. Molecular dynamic simulation

We implement the EMD simulation of methane transport in a parallel-carbon-plate slit-shape pore, which represents the kerogen, to investigate the methane transport behavior in nanopores.

A 3D simulation box is constructed with the length of 30 nm, 4 nm and 2 nm in the x, y and z direction (Figure 1), respectively. The distance between the parallel walls represents the pore diameter of shale, corresponding to the pore-size distribution shown in the next section. Periodic boundary condition is applied on x and z direction, and y-direction is confined by the carbon walls characterized by 10-4-3 potential model with Δ =0.335 nm. For the atoms LJ parameters, we use $\sigma_C = 0.35nm$ and $\varepsilon_C / k_B = 28K$ for carbon atoms, $\sigma_{CH_4} = 0.381nm$ and $\varepsilon_{CH_4} / k_B = 148.1K$ for CH_4 (Cracknell et al. 1995). The Lorentz-Berthelot mixing rules are used to determine the size and energy parameters between the gas molecules and wall atoms (Allen et al. 1989):

$$\sigma_{ij} = \frac{1}{2}\left(\sigma_i + \sigma_j\right) \tag{21}$$

$$\varepsilon_{ij} = \sqrt{\varepsilon_i \varepsilon_j} \tag{22}$$

Then, the parameters for solid-gas interactions of LJ potential are $\sigma_{sf} = 0.3605nm$ and $\varepsilon_{sf} / k_B = 64.4K$. The cut-off distance is $3\sigma_{CH_4}$, and the long-range corrections are not applied. The total number of simulated gas molecules is 682, the temperature is 300.15 K, and the pressure of the system is about 10MPa. We set the time step to be 1 fs and run the simulation for 2000000 steps. The results are shown in Figures 2~3.

Figure 1 shows the simulated domain with snapshots of the molecules for the MD simulation. The blue lines show the location of the parallel carbon walls. Figure 2 reveals that the density distribution indeed exists below the scale of 2 nm from the wall, at which the atoms number density near the surface is much higher than the center part. However, Figure 3 shows that the velocity (self-diffusion) profile is almost flat, which is consistent with the results in Firouzi and Wilcox's (2012) study. Moreover, the observation that the atoms near the solid wall are of a higher number density but have the same total velocity as that of the center indicates that the mass flow near the wall may be larger than the center, resulted from the substantial solid-gas interaction and complex mechanisms.

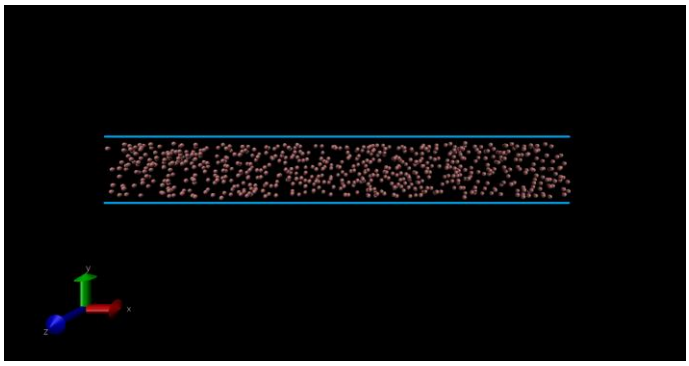

Figure 1 Sketch Map of Simulated Domain (with Snapshots of Molecules)

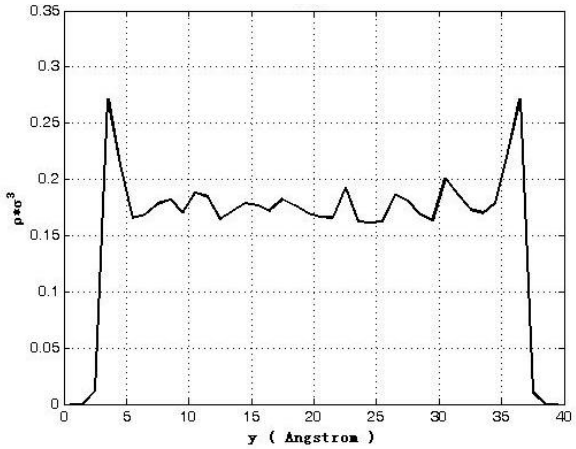

Figure 2 Gas Atom Number Density along Y-Direction

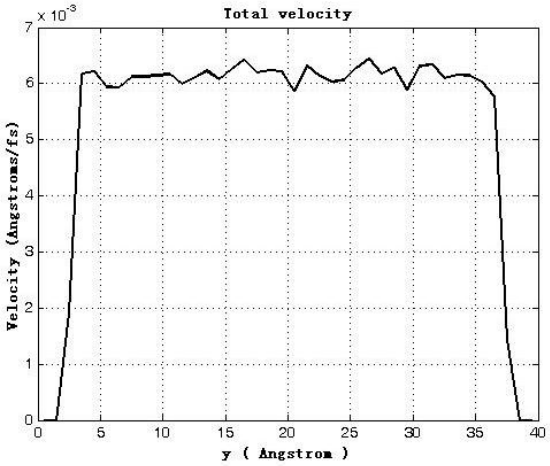

Figure 3 Atoms Averaged Velocity

Although this MD simulation only provides an equilibrium MD case, characterizing the phenomenon of self-diffusion at nanoscale, it shows a totally different mechanism from normal viscous flow with the slip effect and indicates that adsorption may have a greater effect than expected, not only on the mass flow rate but also on the flow regime.

Therefore, the diffusion and adsorption effect must be taken into account for the intrinsic permeability estimation for extremely tight rocks, and further investigation is also required. In this study, we use an existing widely accepted model to determine the intrinsic permeability from experimental data. The nanoscale NEMD simulation under pressure gradient and the effects of diffusion and adsorption on flow regime will be investigated in our future study.

2. Basic petrophysical test

In this study, the rock samples are from the Triassic shale in Ordos basin, China. A series of basic petrophysical tests were performed on the same core samples, which were also crushed, well prepared and dried for more than 24 hours. The petrophysical tests include bulk density and pore size distribution measured by mercury injection capillary pressure (MICP), sample skeleton density and porosity with helium pycnometer, and mineral composition determination with XRD. The results are shown in Table 1 and Figure 4.

Table 1 Basic Petrophysical Parameters Determined from Experimental Tests

Parameters	Results
Porosity	12.58%
Bulk Density	2.1321 g/cm^3
Mineral Composition	Quartz 42.5%
	Albite 33.0%
	Illite 24.5%

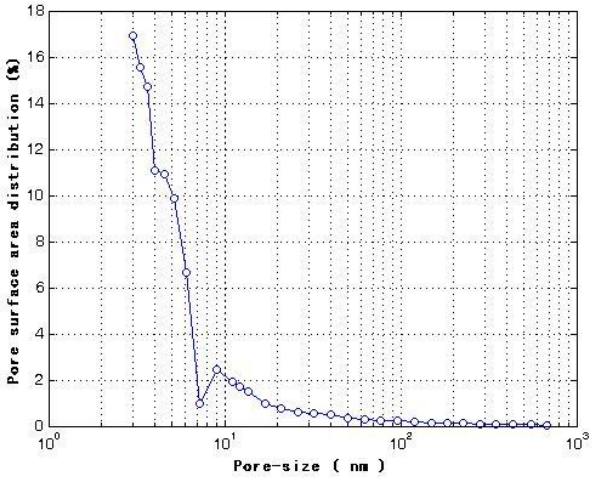

Figure 4 Pore Size Distribution

(Represented by pore surface area distribution)

Since CH_4 and CO_2 are used to perform crushed samples tests, firstly their adsorption isothermals need to be determined experimentally as the input parameters for the permeability calculation. The apparatus is also the same with the Helium pycnometer. We

use Helium to test the open space of the device and the pore space of the sample. Then, the CH_4 and CO_2 adsorption experiments are conducted under different pressures. It is assumed that both CH_4 and CO_2 follow the Langmuir adsorption type. The final Langmuir adsorption isothermal curves for permeability calculation are shown in Figure 5.

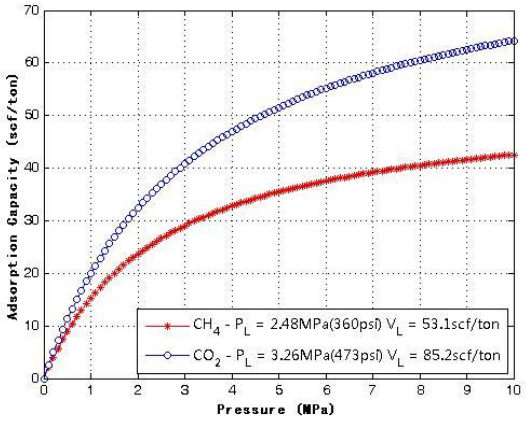

Figure 5 Langmuir Isothermal Curves of Shale Samples

3. Permeability test and interpretation

The permeability tests are conducted under different pressures for a certain sample and interpreted according to the method described in previous section. The intrinsic permeability k, average particle radius R_a and mean hydraulic radius R_h are chosen as fitting parameters and determined by trial and error to match the pressure data. Then, the apparent permeability values for CH_4 and CO_2 under different conditions can be calculated. The best-estimated parameter values are listed in Table 2. The fitted average particle radius is smaller than the expected value, which uses 10/18 mesh (about 1-2 mm) for preparing the crushed sample since the shape of most particles is slice. The mean hydraulic radius corresponds to the pore size distribution shown in Figure 4. Some sets of results are shown in Figure 6 and Figure 7, tested with CH_4 and CO_2, respectively.

Figure 6 indicates that the pressure had two stages of drawdown, in which both late-time and early-time data can be well fitted independently (1.8 nD and 4.2 nD, respectively). However, a good fitting result cannot be achieved for the full range of data. Figure 4 shows that there are two peaks in the pore-size distribution curve, 9nm and less than 3nm, respectively, indicating that the sample may have a similar property as the dual-porous media. One way to interpret this phenomenon is as follow: the gas penetrates the sample through both relatively large and small pores, then the pressure in the large pores reaches the same pressure with the sample cell (outside of the particle), but the pressure gradient still exists between the small pores and large pores. Therefore, pressure decay in the early-time and late-time is dominated by relatively large pores and small pores, respectively.

Table 2 Best-estimated Parameter Values and Calculated Apparent Permeability

	CH_4 (Early-time)	CH_4 (Late-time)	CO_2
Intrinsic Permeability k (nD)	4.2	1.8	3.9
Average Particle Radius R_a (mm)	0.75	0.65	0.75
Mean Hydraulic Radius R_h (nm)	11.5	6.5	11
Representative Apparent Permeability k_a (nD, under 5MPa, 300.15K)	6.3	3.4	6.8

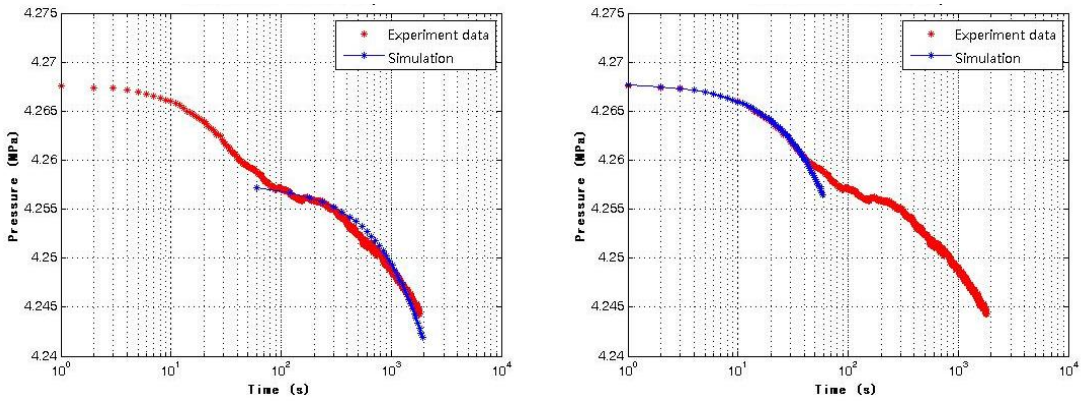

Figure 6 Fitting Results of Permeability Tests with CH_4

(Left: Fit the late-time data only; Right: Fit the early-time data only)

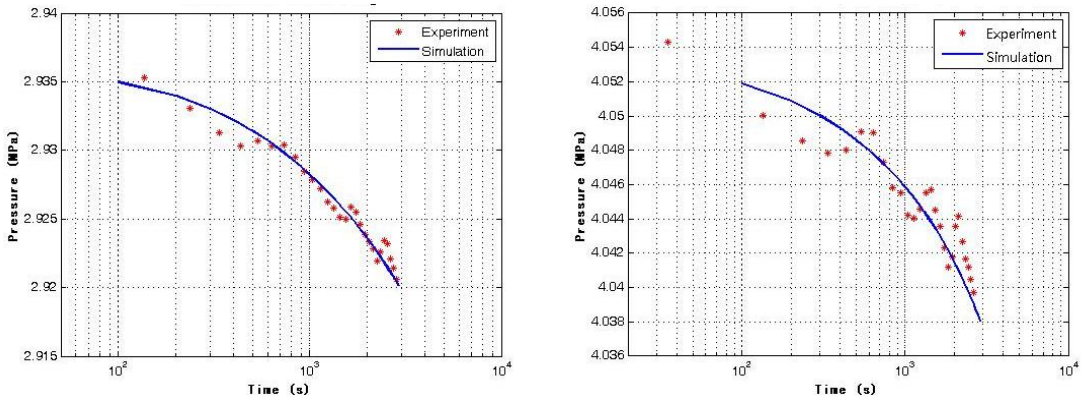

Figure 7 Fitting Results of Permeability Tests with CO_2 for Different Pressures

However, the phenomenon is not observed in the CO_2 test. This is due to the higher apparent permeability of CO_2 than CH_4 (Table 2), so that the early-time behavior like that in CH_4 test cannot be detected or the behaviors have been mixed together. Therefore, further experimental investigation should also focus on providing more various and well-controlled pressure and temperature condition and even shale's microstructure observation.

CONCLUSION

The MD simulation results reveal that the atoms number density near the wall surface is much higher than that in the center part of nanopores due to adsorption, whereas the atoms near the wall has the same order of self-diffusion coefficient with the atoms in the center. This results in a totally different velocity profile, especially near the boundary at the interface of solid and gas. The phenomenon indicates that diffusion and adsorption are critical in nanoscale shale matrix, and may even change the flow regime. Therefore, their effects must be taken into account for the intrinsic permeability estimation for tight rocks and an otherwise simplified model may lead to significant deviation.

Some sets of crushed shale samples have been tested using the transient pulse-decay method. The experimental data are interpreted with a comprehensive model, considering the effects of Knudsen diffusion and adsorption, with the implicit or simulator-based fitting method instead of the traditional analytical approximation method. The interpreted results show that there exists a multi-porous media phenomenon in shale matrix.

REFERENCES

1. Allen, M. P., and D. J. Tildesley. "Computer simulation of liquids, 1987." New York: Oxford 385 (1989).
2. Ambrose, R. J., Hartman, R. C., Diaz-Campos, M., Akkutlu, I. Y., & Sondergeld, C. H. "Shale gas-in-place calculations part I: new pore-scale considerations." *SPE Journal* 17.01 (2012): 219-229.
3. Beskok, Ali, and George Em Karniadakis. "Report: a model for flows in channels, pipes, and ducts at micro and nano scales." *Microscale Thermophysical Engineering* 3.1 (1999): 43-77.
4. Civan, Faruk, Chandra S. Rai, and Carl H. Sondergeld. "Determining shale permeability to gas by simultaneous analysis of various pressure tests." *SPE Journal* 17.03 (2012): 717-726.
5. Civan, Faruk, Chandra S. Rai, and Carl H. Sondergeld. "Shale-gas permeability and diffusivity inferred by improved formulation of relevant retention and transport mechanisms." *Transport in Porous Media* 86.3 (2011): 925-944.
6. Civan, Faruk. "Effective correlation of apparent gas permeability in tight porous media." *Transport in Porous Media* 82.2 (2010): 375-384.
7. Cracknell, Roger F., David Nicholson, and Nicholas Quirke. "Direct molecular dynamics simulation of flow down a chemical potential gradient in a slit-shaped micropore." *Physical Review Letters* 74.13 (1995): 2463.
8. Cui, X., A. M. M. Bustin, and Robert M. Bustin. "Measurements of gas permeability and diffusivity of tight reservoir rocks: different approaches and their applications." *Geofluids* 9.3 (2009): 208-223.
9. Dicker, A. I., and R. M. Smits. "A practical approach for determining permeability from laboratory pressure-pulse decay measurements." *International Meeting on Petroleum Engineering*. Society of Petroleum Engineers, SPE-17578, 1988.

10. Egermann, P., Lenormand, R., Longeron, D. G., & Zarcone, C. "A fast and direct method of permeability measurements on drill cuttings." *SPE Reservoir Evaluation & Engineering* 8.04 (2005): 269-275.
11. Firouzi, Mahnaz, and Jennifer Wilcox. "Molecular modeling of carbon dioxide transport and storage in porous carbon-based materials." *Microporous and Mesoporous Materials* 158 (2012): 195-203.
12. Firouzi, Mahnaz, and Jennifer Wilcox. "Slippage and viscosity predictions in carbon micropores and their influence on CO_2 and CH_4 transport." *The Journal of chemical physics* 138.6 (2013): 064705.
13. Javadpour, Farzam. "Nanopores and apparent permeability of gas flow in mudrocks (shales and siltstone)." *Journal of Canadian Petroleum Technology* 48.8 (2009): 16-21.
14. Jones, S. C. "A technique for faster pulse-decay permeability measurements in tight rocks." *SPE Formation Evaluation* 12.01 (1997): 19-26.
15. Kundert, Donald P., and Michael J. Mullen. "Proper evaluation of shale gas reservoirs leads to a more effective hydraulic-fracture stimulation." S*PE Rocky Mountain Petroleum Technology Conference.* Society of Petroleum Engineers, SPE-123586, 2009.
16. Luffel, D. L., C. W. Hopkins, and P. D. Schettler Jr. "Matrix permeability measurement of gas productive shales." *SPE Annual Technical Conference and Exhibition*. Society of Petroleum Engineers, SPE-26633, 1993.
17. Sakhaee-Pour, Ahmad, and Steven Bryant. "Gas permeability of shale." *SPE Reservoir Evaluation & Engineering* 15.04 (2012): 401-409.
18. Skoulidas, A. I., Ackerman, D. M., Johnson, J. K., & Sholl, D. S. "Rapid transport of gases in carbon nanotubes." *Physical Review Letters* 89.18 (2002): 185901.
19. Sondergeld, Carl H., et al. "Micro-structural studies of gas shales." *SPE Unconventional Gas Conference*. Society of Petroleum Engineers, SPE-131771, 2010.
20. Steele, William A. The interaction of gases with solid surfaces. Vol. 3. Oxford: Pergamon Press, 1974.
21. Tang, G.H., Tao, W.Q., He, Y.L. "Gas slippage effect on microscale porous flow using the lattice Boltzmann method." *Phys. Rev. E* 72.8 (2005): 056301.
22. Zhang, H., Zhang, Z., Zheng, Y., & Ye, H. "Corrected second-order slip boundary condition for fluid flows in nanochannels." *Physical Review E* 81.6 (2010): 066303.
23. Zhu, G. Y., Liu, L., Yang, Z. M., Liu, X. G., Guo, Y. G., & Cui, Y. T. "Experiment and Mathematical Model of Gas Flow in Low Permeability Porous Media." *New Trends in Fluid Mechanics Research*. Springer Berlin Heidelberg, (2009). 534-537.
24. Ziarani, Ali S., and Roberto Aguilera. "Knudsen's permeability correction for tight porous media." *Transport in Porous Media* 91.1 (2012): 239-260.